
How feedback inhibition shapes Spike-Timing-Dependent Plasticity

Anonymous Author(s)

Affiliation

Address

email

Abstract

It has been shown that plasticity is not a fixed property but, in fact, changes depending on the location of the synapse on the neuron and/or changes in biophysical parameters. Here we investigate how plasticity is shaped by the microcircuit around a neuron. In particular we focus on the feedback inhibition which exerts a strong influence on the neuronal dynamics and consequently on the underlying plasticity. We use a differential Hebbian learning rule to model spike-timing-dependent plasticity and show analytically that the feedback inhibition alters the time window for LTD but not for LTP. These analytical results are then enhanced by realistic simulations which suggest that not only the shape of LTD is altered but that its magnitude is less under the influence of feedback inhibition. This provides a possible explanation for the observed hypofrontality in schizophrenia where feedback inhibition is weak.

1 Introduction

Spike-timing-dependent plasticity [1, 2, 3] is a special form of Hebbian learning [4] where the order of the pre- and postsynaptic events determine weight growth or decay. Plotting different timings between pre- and postsynaptic potentials leads to the so-called STDP curve. It has been shown recently that this STDP curve is not constant but changes its shape when the pre- and postsynaptic potentials change. To reflect this we have developed a learning rule which *generates* the STDP curve on the basis of biophysical parameters rather than defining it rigidly. Put simply, this learning rule employs differential Hebbian learning by correlating the NMDA activation with the derivative of the postsynaptic potential or concentration (e.g. Calcium).

We have shown that backpropagating spikes can change the shape of the STDP curve and that distal dendrites have their own STDP curves. This is because local calcium spikes behave somewhat Hebbian. Postsynaptic potentials, however, are not only changed by intrinsic properties, such as distance from the soma, but also by external influences from the surrounding neural network. In this paper we explore how the feedback inhibition changes the STDP curve. The feedback inhibition in a cortical microcircuit has a strong effect on the pyramidal neuron by resetting the membrane potential quickly to the resting potential (shunting inhibition). Consequently, the shape of the STDP curve will be altered in the presence of the interneuron. We will show that feedback inhibition changes the shape of the STDP curve in a way that LTD is happening only in a short time window and that strong inhibition causes less LTD. This result is a possible explanation for the observed depression in the prefrontal cortex after chronic application of the NMDA receptor antagonist PCP, a recent model for schizophrenia. Thus, we propose that less inhibition in the cortical microcircuit causes more LTD and could be a possible explanation of the hypofrontality in schizophrenia. We will first derive the STDP curve analytically and then go on to show results from a more realistic simulation.

2 Analytical derivation of STDP with Feedback Inhibition

We will now show analytically that inhibitory feedback influences the STDP curve in a very specific way, namely that it changes the *shape* of the negative part of the STDP curve ($T < 0$) while the positive part ($T > 0$) is scaled only. In order to achieve an analytical result we need to switch to the Laplace domain which allows a simple treatment of the feedback loop.

Fig. 1B shows the formalised circuit diagram of the cortical microcircuit (Fig. 1A) where we have switched to the Laplace domain. The model was designed using the GENESIS-sim software [5] and consists of a cortical pyramidal cell and attached interneuron. Looking at Fig. 1A we can see the excitatory “input” which is the modelled presynaptic input into the pyramidal cell. The modelled action potential is simply a delta impulse function, $\Delta(t)$. Attached to the pyramidal cell are AMPA and NMDA receptors which will be discussed in the next section. A current injection into the pyramidal cell stimulates the neuron enough to generate the postsynaptic action potential. This propagates to the pyramidal cell body down through the axon activating the NMDA receptors on the GABAergic interneuron, allowing an influx of Ca^{2+} into the cell. If the excitation is strong enough the interneuron releases GABAergic neurotransmitters back to the pyramidal cell, inhibiting as it does so. Both the pyramidal cell and interneuron use the Hodgkin-Huxley model [6] to implement ionic conductances realistically.

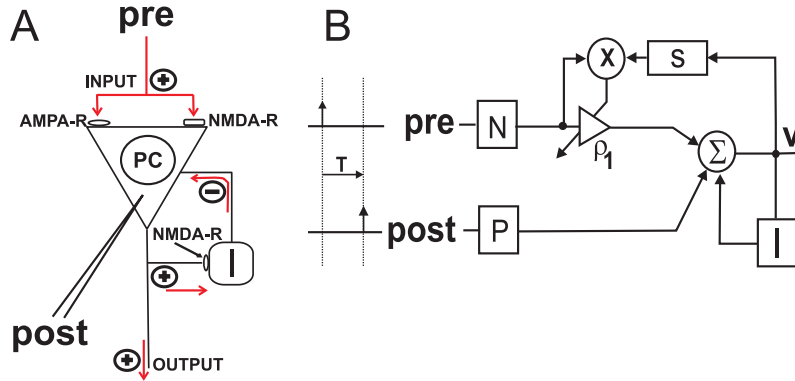


Figure 1: A: Graphical representation of model designed using the GENESIS-sim software [5]. “pre” is the excitatory “input”, a modelled presynaptic input into the pyramidal cell. Attached to the pyramidal cell are AMPA and NMDA receptors. “post” represents the current injection into the pyramidal cell stimulating the neuron into inducing a postsynaptic action potential. If the excitation is strong enough the interneuron releases GABAergic neurotransmitters back to the pyramidal cell, inhibiting as it does so. Both the pyramidal cell and interneuron use the Hodgkin-Huxley model to implement ionic conductances realistically and detailed calcium dynamics have been used, which will be discussed in the next section. B: Block diagram. The symbol Σ represents a summation node and \otimes multiplication. N is the presynaptic input, the transfer function of the NMDA channel and P being the postsynaptic input, the transfer function of the postsynaptic potential. I is the feedback inhibition, which can be compared to the inhibitory interneuron “I” seen in Fig 1A, and s is the derivative of the postsynaptic potential in the Laplace domain.

The NMDA channel is modelled as:

$$N(s) = \frac{1}{(s + \tau_{N1})(s + \tau_{N2})} \Leftrightarrow n(t) = \frac{1}{\tau_{N1} - \tau_{N2}} (e^{-\tau_{N1}t} - e^{-\tau_{N2}t}) \quad (1)$$

where τ_{N1} and τ_{N2} are rise- and decay-constants of the NMDA channel. The postsynaptic potential is modelled in the same way where we have τ_{P1} and τ_{P2} for the rise and fall times.

$$N(s) = \frac{1}{(s + \tau_{P1})(s + \tau_{P2})} \Leftrightarrow n(t) = \frac{1}{\tau_{P1} - \tau_{P2}} (e^{-\tau_{P1}t} - e^{-\tau_{P2}t}) \quad (2)$$

The feedback inhibition performed via the interneuron is modelled as a first order system to keep the complexity of the solution simple. Although fast spiking interneurons react virtually instantly, they tend to have a long IPSP time [7], mediating the GABAergic release and thus meaning the first order system being a suitable model. The feedback inhibition is as follows:

$$I(s) = \frac{g}{s + \tau_I} \Leftrightarrow i(t) = ge^{-\tau_I t} \quad (3)$$

where g is the gain of the feedback loop and τ_I the decay constant.

The total membrane potential is calculated in the following way:

$$V(s) = \rho_1 N(s) + P(s) - I(s)V(s) \quad (4)$$

where the function $P(s)$ models the postsynaptic response, the function $N(s)$ is the dynamic of the NMDA channel and $I(s)$ the transfer function of the inhibitory neuron, hence the negative sign used.

We can now solve this equation for the membrane potential $V(s)$:

$$V(s) = \frac{\rho_1 N(s) + P(s)}{1 + I(s)} \quad (5)$$

Spike-timing-dependent plasticity is modelled by the product of the NMDA conductance $N(s)$ with the derivative of the postsynaptic potential. The correlation in the Laplace domain is expressed as:

$$\Delta\rho = \int_{-\infty}^{\infty} N(-s)e^{-sT}V(s)ds \Leftrightarrow \Delta\rho = \int_0^{\infty} n(t)v'(t-T)dt \quad (6)$$

Here, we assume that this postsynaptic potential is solely the membrane potential. In the next section we will go on to show simulation results where this has been replaced by the change of the calcium concentration. Substituting Eq's 3 and 5 into Eq. 6 yields an integral which can be solved with the method of residuals. For $T > 0$ the solution is:

$$\Delta\rho(T) = \frac{\tau_{N2}(\tau_{N2} + \tau_I)e^{-\tau_{N2}T}}{(\tau_{N1} - \tau_{N2})(\tau_{N2} + \tau_{P1})(\tau_{N2} + \tau_{P2})(\tau_{N2} + \tau_I + g)} \quad (7)$$

$$- \frac{\tau_{N1}(\tau_{N1} + \tau_I)e^{-\tau_{N1}T}}{(\tau_{N1} - \tau_{N2})(\tau_{N1} + \tau_{P1})(\tau_{N1} + \tau_{P2})(\tau_{N1} + \tau_I + g)} \quad (8)$$

where we see that the timing of the STDP curve is determined by the NMDA channel dynamics (rise and decay times, τ_{N1} and τ_{N2}).

For $T < 0$ the solution looks similar but with the difference that this part of the curve is determined by the postsynaptic dynamics (rise and decay times, τ_{P1} and τ_{P2}):

$$\Delta\rho(T) = \frac{\tau_{P1}(\tau_{P1} - \tau_I)e^{-\tau_{P1}T}}{(\tau_{N1} + \tau_{P1})(\tau_{N2} + \tau_{P1})(\tau_{P1} - \tau_{P2})(\tau_{N1} - \tau_I - g)} \quad (9)$$

$$- \frac{\tau_{P2}(\tau_{P2} - \tau_I)e^{-\tau_{P2}T}}{(\tau_{N1} + \tau_{P2})(\tau_{N2} + \tau_{P2})(\tau_{P1} - \tau_{P2})(\tau_{N2} - \tau_I - g)} \quad (10)$$

$$+ \frac{g(\tau_I + g)e^{(\tau_I + g)T}}{(\tau_{N1} + \tau_I + g)(\tau_{N2} + \tau_I + g)(\tau_{P1} - \tau_I - g)(\tau_{P2} - \tau_I - g)} \quad (11)$$

The third term (11) arises from the inhibitory feedback. This term becomes strong against the other two terms if the gain ' g ' is high and/or if the time constant of the feedback is similar to the time constants of the postsynaptic potential.

Fig. 2 shows the results for strong feedback (A) and weak feedback (B). It is observed that the shape of the STDP curve is altered for $T < 0$ while the positive part $T > 0$ is scaled only. With stronger inhibition, LTD is confined to a small time window of around 20ms, while the weaker inhibition gives a much wider window of about 50ms. This means that stronger feedback inhibition generates a much more precise time window for LTD than when there is no inhibition. Note that because of the nature of the functions used, the ratio of LTP and LTD always equals one which causes the scaling of the LTP part.

For that reason we will now discuss a more realistic scenario which shows that feedback inhibition does indeed change the ratio of LTP and LTD when these mechanisms are controlled by independent coincidence detectors. In the realistic scenario we continue to observe the previous result from the analytics; only the negative part of the STDP curve is modulated by the feedback inhibition.

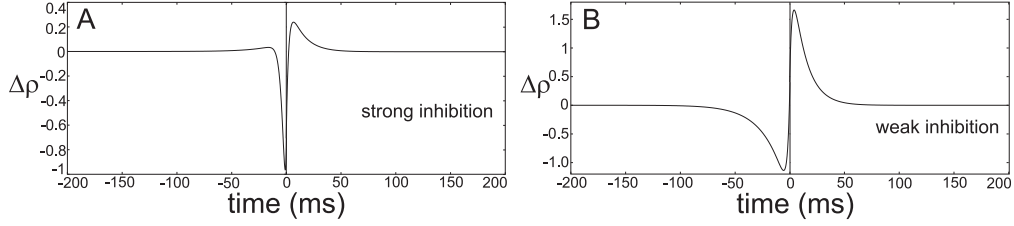


Figure 2: Spike timing dependent plasticity curves with strong and weak feedback inhibition. In curve A, the inhibitory feedback has a high gain. This results in the postsynaptic potential during $T < 0$ to be significantly reduced, and this is reflected when looking at the shorter time period that LTD is present as well as its shape being clearly reduced. For $T > 0$, the shape of the curve remains, although is at a smaller ratio due to the nature of the integration. B: When there is a low gain from the inhibitory feedback, we observe the typical STDP curve.

3 Realistic Model of STDP with Feedback Inhibition

As previously discussed, the microcircuit model used was created using a custom-compiled version of the GENESIS-sim 2.3 modelling tool [5] (<http://www.GENESIS-sim.org/GENESIS>) and consists of a modelled cortical pyramidal cell and attached GABAergic inhibitory interneuron (Fig. 1A).

Using the GENESIS-sim modelling tool [5], we were able to create a modelled cortical pyramidal cell with Hodgkin-Huxley dynamics [6] to include the active properties of the cell membrane along with modelling detailed calcium dynamics, AMPA and NMDA receptors.

In this realistic case, there are two coincidence detectors: one for LTP and one for LTD. It is known that the strength in plasticity-change is greatly affected by the influx of Ca^{2+} into postsynaptic NMDA receptors [8, 9]. For the modelling of the LTP part of the curve (when the postsynaptic potential derivative is greater than zero), we have used the product of the NMDA-R activation and the derivative of the intracellular calcium concentration, $[\text{Ca}^{2+}]'_i$.

To model the cellular mechanisms taking place during synaptic depression, we refer to a study by Tanaka et al [10], who proposed that the relationship between calcium dynamics and the decline in synaptic strength can be modelled using a leaky integrator. We therefore model the second coincidence detector using the filtered derivative of the calcium outflux ($h_{\tau_{\text{Ca}^{2+}}} * \Theta(-[\text{Ca}^{2+}]'_o)$).

3.1 NMDA receptor dynamics

An NMDA receptor has been created which updates the weight change of AMPA synapses based on the NMDA receptor activation [8]. Hence, by adding parameters which control the timing of the NMDA receptor activation, we can directly affect Ca^{2+} flow into and out of the postsynapse.

The NMDA-R conductance depends on the cell membrane potential, V_m , as well as being dependent on Magnesium, which obstructs the NMDA-R until the cell becomes depolarised and allows the receptor to become permeable to Na^+ , K^+ and Ca^{2+} ions. The NMDA conductance is calculated using [11]:

$$g_{\text{NMDA}}(t) = \bar{g} \frac{e^{-\frac{t}{\tau_1}} - e^{-\frac{t}{\tau_2}}}{1 + \eta[\text{Mg}^{2+}]e^{-\gamma V_m}} \quad (12)$$

with rise and decay times $\tau_1 = 2$ ms, $\tau_2 = 100$ ms and maximal conductance, \bar{g} . The Magnesium-block parameters are: $\gamma = 0.06/\text{mV}$, $\eta = 0.33/\text{mM}$ and magnesium concentration, $[\text{Mg}^{2+}] = 2\text{mM}$.

This can be directly compared to the analytical solution of the NMDA receptor gating (τ_1 and τ_2 being comparable to rise times τ_{N1} and τ_{N2}). The lifting of the Magnesium-block is dependent on the change of the cell's membrane potential, therefore the decay constant term $e^{-\gamma V_m}$ describes how quickly the Mg^{2+} -block is resolved.

3.2 Calcium Dynamics

The calcium model used was a Low-Threshold calcium current, I_T , by Destexhe et al [12] and is as follows:

$$\begin{aligned} I_T &= \bar{g}_{Ca^{2+}} m^2 h (V - E_{Ca^{2+}}) \\ \dot{m} &= -\frac{1}{\tau_m(V)} [m - m_\infty(V)] \\ \dot{h} &= -\frac{1}{\tau_h(V)} [h - h_\infty(V)] \end{aligned}$$

$\bar{g}_{Ca^{2+}} = 1.75$ mS/cm² and is the maximum conductance value of the calcium current, V is the cell membrane potential, $E_{Ca^{2+}}$ the reversal potential. m and h are the activation and inactivation variables and their functions and time constants are calculated from:

$$\begin{aligned} m_\infty(V) &= \frac{1}{1 + e^{-\frac{V+52}{7.4}}} \\ \tau_m(V) &= 0.44 + \frac{0.15}{e^{\frac{V+27}{10}} + e^{-\frac{(V+102)}{15}}} \\ h_\infty(V) &= \frac{1}{1 + e^{\frac{V+80}{5}}} \\ \tau_h(V) &= 22.7 + \frac{0.27}{e^{\frac{V+48}{4}} + e^{-\frac{V+407}{50}}} \end{aligned}$$

The values have been calculated for a temperature of 36°C.

In the GENESIS-sim [5] model, the change in calcium concentration is calculated from a single-pool exponential:

$$dCa^{2+}/dt = B \cdot I_{Ca^{2+}} - Ca^{2+}/\tau \quad (13)$$

modelling the low-threshold calcium current, $I_{Ca^{2+}}$, with parameters: $\bar{g}_{Ca^{2+}} = 1.75$ mS/Cm², decay-time $\tau_{Ca^{2+}} = 30$ ms, $[Ca^{2+}]_i = 2$ mM/litre. $B = 1e12$ (1 / calcium charge ($C_{Ca^{2+}}$) multiplied by the Faraday constant multiplied by the ion shell volume).

Ca^{2+} is the resulting concentration of the calcium ions and Ca_{base}^{2+} is the base-level concentration, giving $Ca^{2+} = Ca_{base}^{2+} + Ca^{2+}$.

3.3 The Learning Rule

The derivative of the postsynaptic potential $[Ca^{2+}]'$ is split into two parts. The first,

$$g_{NMDA}(t) \cdot \Theta([Ca^{2+}]'_i) \quad (14)$$

is for $[Ca^{2+}]'_i > 0$, when there is an influx of Ca^{2+} into the receptor. We can compare $[Ca^{2+}]'_i$ to the derivative of the postsynaptic potential from the analytical solution, $P(s)$, and the receptor activation, $NMDA_{act}$ to $G(s)$.

The second term:

$$g_{NMDA}(t) \cdot h_{\tau_{Ca^{2+}}} * \Theta(-[Ca^{2+}]'_o) \quad (15)$$

describes when the derivative of the postsynaptic potential ($[Ca^{2+}]'_o < 0$). That is, the outflux of the Ca^{2+} from the receptor, hence the negative part being represented. $h_{\tau_{Ca^{2+}}}$ describes the first-order lowpass filtering of the calcium concentration derivative. We have chosen the time constant of the filter, $\tau_{Ca^{2+}} = 0.8$ ms, as this gives the most realistic output during STDP simulation runs. We can now write the collective learning rule as

$$\Delta\rho = \mu \cdot g_{NMDA}(t) \cdot \Theta([Ca^{2+}]'_i) - \gamma \cdot g_{NMDA}(t) \cdot h_{\tau_{Ca^{2+}}} * \Theta(-[Ca^{2+}]'_o) \quad (16)$$

where $\Delta\rho$ is the update in synaptic weight. If we then go on to set $h_{\tau_{Ca^{2+}}} = 1$, $\mu = 1$ and $\gamma = 1$, we observe that we are able to get back to equation 6.

3.4 Results

In the simulation run, we have a fixed-time presynaptic input, I_0 (a modelled action potential, $\delta(t)$), and the postsynaptic input, a variable-timed current injection, I_1 . The difference in timing between the fixed input I_0 and variable postsynaptic input, I_1 , is known as T , or the ‘‘Interspike interval’’. As mentioned in Figure 1A, the attached interneuron is a modelled GABAergic cell with NMDA and GABA receptors, along with detailed HH-channels [6].

We have chosen the filter decay constant ‘ $h_{\tau_{Ca^{2+}}}$ ’ (0.8 ms) which allows for the most biologically accurate output [10]. The weight change, $\Delta\rho$, is plotted against the interspike interval, T . The two simulations (with and without the feedback inhibition/inhibitory interneuron) are seen in Fig. 3B. Observing the STDP curve when feedback inhibition/inhibition is performed by the interneuron (Fig. 3B - dashed line) compared to without (Fig. 3B - solid line), it is interesting to note the decline in magnitude *and* shape of the LTD window, while long-term potentiation remains the same. We can draw comparisons between the analytical model and our more realistic model when looking at this reduced time window for LTD (Fig. 2A). This is due to the dual nature of the GABAergic interneuron. It was found by Aihara [13] and also explained by Edward O’ Mann [14] that fast spiking GABAergic interneurons cause a phenomenon known as ‘‘shunting inhibition’’ on the pyramidal cell [14]. GABA receptors are connected to chloride channels (Cl^-) which have a reversal potential near to that of the resting membrane potential of the pyramidal cell ($E_{Cl^-} = E_{rest} = -65mV$) causing the shunting inhibition. Doiron et al [15] show that during subthreshold frequencies (10Hz - 15Hz), shunting gain control acts divisive in nature. The GABAergic effects of the interneuron division-operation can be seen directly in Figure. 3B as diminished magnitude and shaping of the LTD part of the STDP curve. Thus, when comparing to the analytical solution on the previous section, we can see similarities in the change in curve shape ($T < 0$) while the LTP ($T > 0$) remains the same shape (Fig. 2A and Fig. 3B - dashed line).

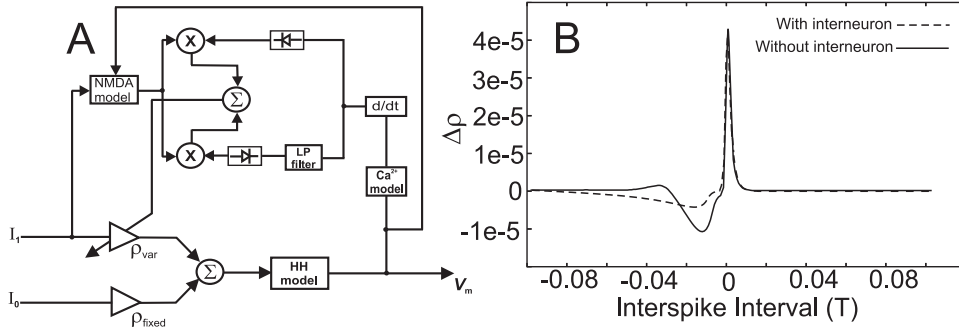


Figure 3: A: Block Diagram of STDP learning rule used. I_1 represents the variable spiking-event (current injection) timing, which can be altered to give either LTD or LTP depending on its occurrence before or after the fixed input, I_0 . These two inputs are summated to give the timing difference between post and presynaptic spiking, T . In both parts of the learning rule there are HH ion channels and detailed calcium dynamics modelled. For both LTP and LTD, the derivative of the calcium concentration, $[Ca^{2+}]_i$ is found. For LTP, the positive derivative of the $[Ca^{2+}]_i$ is taken. For LTD, the derivative is put through a lowpass leaky-integrator filter before taking the negative derivative of this. Both the positive and negative derivatives are dependent on NMDA-receptor activation which will affect the change in plasticity. B: Comparison between STDP plots of pyramidal cell with (dashed line) and without (solid line) interneuron, both using $\tau = 0.8$ ms. By comparing the STDP curve with attached interneuron to without interneuron (dashed line), a distinct decrease in magnitude and shape of the curve is seen.

4 Discussion

The classical model of spike-timing-dependent plasticity measures the temporal distance between pre- and postsynaptic potentials and then looks up the weight change in a predefined function. This generally is either created specifically, or is derived from rather computational principles like the ‘‘spike response’’ model [16]. In our case the STDP curve emerges simply by integrating the learning rule (Eq. 6) which is based on biophysical parameters. The obvious advantage of this is that we are

not limited to two discrete time events (e.g. pre- and postsynaptic spike) but can actually calculate STDP in a network with many inputs. This is especially true in our model where we have three events occurring; the presynaptic input, the postsynaptic input and then the third being the inhibitory feedback from the interneuron.

In our model both LTP and LTD are determined by the postsynaptic potential derivative (or calcium concentration derivative in the realistic model) in the learning rule. We propose that the influx of Ca^{2+} through the NMDA receptor causes LTP and that the outflux of Ca^{2+} ions cause LTD. It has been shown experimentally and theoretically that LTP is caused by a transient *change* in the calcium concentration [17]. Modelling LTD based on the Ca^{2+} outflux has been recently proposed by Tanaka where the STDP curve could be constructed from the “velocity” (derivative) of the calcium concentration flowing out of the NMDA receptors.

We have shown that it is possible to model the relationship between Ca^{2+} dynamics and LTD, as stated by Tanaka [10]. This implies that the leaky integrator mechanism could realistically be a postsynaptic cell mechanism responsible for LTD.

We know that hypofrontality is a condition seen in patients with schizophrenia and with our model we put forward the hypothesis that reduced inhibition in the cortical microcircuit will result in a higher magnitude of LTD present. With this, we suggest the longer time window in which LTD is seen could be a possible explanation for this hypofrontality.

References

- [1] H. Markram, J. Lübke, M. Frotscher, and B. Sakman. Regulation of synaptic efficacy by coincidence of postsynaptic APs and EPSPs. *Science*, 275:213–215, 1997.
- [2] J. C. Magee and D. Johnston. A synaptically controlled, associative signal for Hebbian plasticity in hippocampal neurons. *Science*, 275:209–213, 1997.
- [3] Guo-qiang Bi and Mu-ming Poo. Synaptic modifications in cultured hippocampal neurons: Dependence on spike timing, synaptic strength, and postsynaptic cell type. *J. Neurosci.*, 18(24):10464–10472, 1998.
- [4] D. O. Hebb. *The organization of behavior: A neuropsychological theory*. Wiley-Interscience, New York, 1949.
- [5] J.M. Bower and D. Beeman. *The Book of GENESIS: Exploring Realistic Neural Models with the GENeral NEural Simulation System (2nd Ed.)*. Springer-Verlag, New York, 1998.
- [6] A.L.Hodgkin and A.F.Huxley. A quantitative description of membrane current and its application to conduction and excitation in nerve. *J.Physiol*, 17(4):500–544, 1952.
- [7] A. V. Zaitsev, N.V. Povysheva, D. A. Lewis, and L. S Krimer. P/Q-Type, But Not N-Type, Calcium Channels Mediate GABA Release From Fast-Spiking Interneurons to Pyramidal Cells in Rat Prefrontal Cortex. *J Neurophysiol*, 97:3567–3573, 2007.
- [8] J. Lisman. The cam kinase II hypothesis for the storage of synaptic memory. *Trends Neurosci.*, pages 406–412, 1994.
- [9] T. G. Oerthner B. L. Sabatini and K. Svoboda. The life cycle of Ca^{2+} ions in dendritic spines. *Neuron*, 33:439–452, 2002.
- [10] K. Tanaka, L. Khiroug, F. Santamaria, T. Doi, H. Ogasawara, G. C. R. Ellis-Davies, M. Kawato, and G. J. Augustine. Ca^{2+} requirements for cerebellar long-term synaptic depression: Role for a postsynaptic leaky integrator. *Neuron*, 54:787–800, June 2007.
- [11] C. Koch (Ed). *Biophysics of Computation: Information Processing in Single Neurons*. Oxford University Press, New York USA, 1998.
- [12] A. Destexhe, D. Contreras, T. J. Sejnowski, and M. Steriade. A Model of Soindle Rhythmicity in the Isolated Thalamic Reticular Nucleus. *Journal of Neurophysiology*, 2:803–818, 1994.
- [13] T. Aihara, Y. Yamazaki Y. Abiru, Y. Fukushima H. Watanabe, and M. Tsukada. The relation between spike-timing dependent plasticity and Ca^{2+} dynamics in the hippocampal CA1 network. *Neuroscience*, 145:80–87, 2007.
- [14] E. O’Mann and O. Paulsen. Keeping Inhibition Timely. *Neuron*, 49(1):8–9, 2006.

- [15] B. Doiron, N. Berman A. Longtin, and L. Maler. Subtractive and Divisive Inhibition: Effect of Voltage-Dependent Inhibitory Conductances and Noise. *Neural Computation*, 13:227–248, 2000.
- [16] R. Jolivet, T. Lewis, and W. Gerstner. The Spike Response Model: A framework to predict neuronal spike trains, 2003.
- [17] M. Lindskog, M. S. Kim, M.A. Wikstrom, K. T. Blackwell, and J. Hellgren Kotaleski. Transient calcium and dopamine increase PKA activity and DARPP-32 phosphorylation. *PLoS Comput Biol*, 2:1045–1060, 2006.